Molecular conductance

Valkenier-van Dijk, Elisabeth Hendrica

Chapter 1
Molecular Electronics

This chapter introduces our Matrix Approach to study the molecular conductance of π-conjugated wires and switches. We explain the opportunities of conjugation topologies for molecular electronics and describe various methods by which molecular conductance can be studied.

1.1 Introduction

Life has changed significantly in the last centuries. Thanks to inventions of for instance engines and electric lightning during the 19th century, products are no longer made by hand but mechanically crafted in large factories, transportation became easier, as did life at home. After the industrial revolution, the 20th century saw an electronic revolution to such a point that life without computers or internet is unimaginable. Current developments are the miniaturization of electronics and the replacement of classical semiconductors as silicon, germanium, and gallium arsenide by organic materials in so-called "organic electronics". In this thesis we will combine both these developments and we will investigate the potential use of single organic molecules (or a single layer of molecules) in electronics,[1] aptly called "Molecular Electronics".[2] The ultimate aim would be to construct electronic circuits of molecules only.[3] In Section 1.3 we present how molecules could be wired and how logic operations could be performed with these molecules, in theory. However, in experiments we cannot go that far yet. Even the conductance measurements on single molecules are not trivial and subject of debate. Therefore, we investigate the electrical conductance properties of molecules by integrating these molecules in metal-molecule-metal junctions, as we describe in Section 1.4. By studying series of molecules in different metal-molecule-metal junctions, as shown in Section 1.5 we aim at finding the influence of molecular structure on the electrical conductance. We will first introduce the type of molecules this thesis deals with: π-conjugated molecules.

1.2 π-Conjugated Molecules in Organic Electronics

The molecules and polymers shown in Figure 1.1 are important in organic electronics and are used in commercially available organic solar cells or other organic devices. These structures have in common that they are made-up almost entirely of π-conjugated carbon frames, which can be recognized in these drawings by their double and single bonds. It is this π-conjugation which gives the molecules their semi-conducting properties.

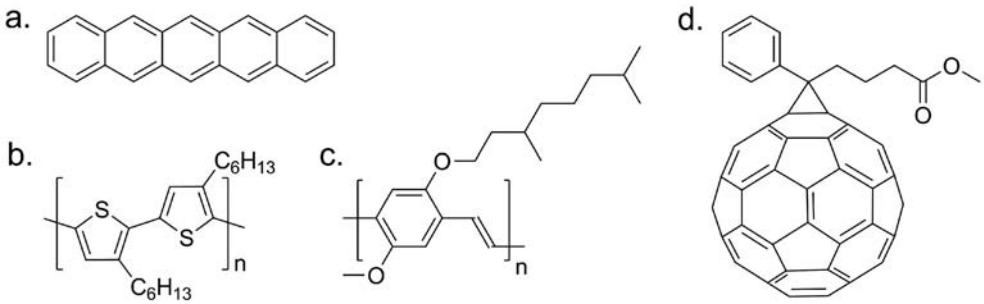

Figure 1.1 Examples of conjugated molecules and polymers that are applied in organic electronics: **a.** pentacene, **b.** regioregular poly(3-hexylthiophene) (P3HT), **c.** a poly(phenylene vinylene) (MDMO-PPV), and **d.** [6,6]-phenyl-C_{61}-butyric acid methyl ester (PCBM).

The description of π-conjugation as a pattern of alternating single and double bonds is based on valence-bond theory. An alternative way of considering bonding in molecules is molecular orbital theory, which states that the atomic orbitals of the atoms in a molecule are combined to form the same number of molecular orbitals. Energy is gained with this combination when the symmetry of the orbitals allows overlap and a bond is formed. The molecular orbitals that are the lowest in energy are in general related to the σ-bonds (which hold the atoms together).

Carbon atoms have four electrons in the four valence atomic orbitals: 2s, $2p_x$, $2p_y$, and $2p_z$. These atomic orbitals hybridize when involved in the formation of a σ-bond. The carbon atoms in the π-conjugated cores of the molecules in Figure 1.1 are sp^2 hybridized: the 2s, $2p_x$, and $2p_y$ mix to form three sp^2-orbitals, which are involved in σ-bonds. The p_z-orbitals, that are oriented perpendicular to the σ-bonds, remain and can combine to form molecular orbitals, as shown for ethene in Figure 1.2a. The "bonding molecular orbital" corresponds to a π-bond (the second line of each double bond in Figure 1.1). The gain in energy from the formation of a π-bond is much smaller than for a σ-bond.

The (opto)electronic properties of molecules are dominated by their frontier orbitals: the highest occupied molecular orbital (HOMO) and the lowest unoccupied molecular orbital (LUMO). Since the bonding orbitals that are composed from p_z-orbitals are in general higher in energy than those involved in σ-bonds and the corresponding (unoccupied) anti-bonding molecular orbitals are relatively low in energy (compared to anti-bonding σ-orbitals), the HOMO and the LUMO of conjugated molecules are constructed from linear combinations of the p_z-orbitals.

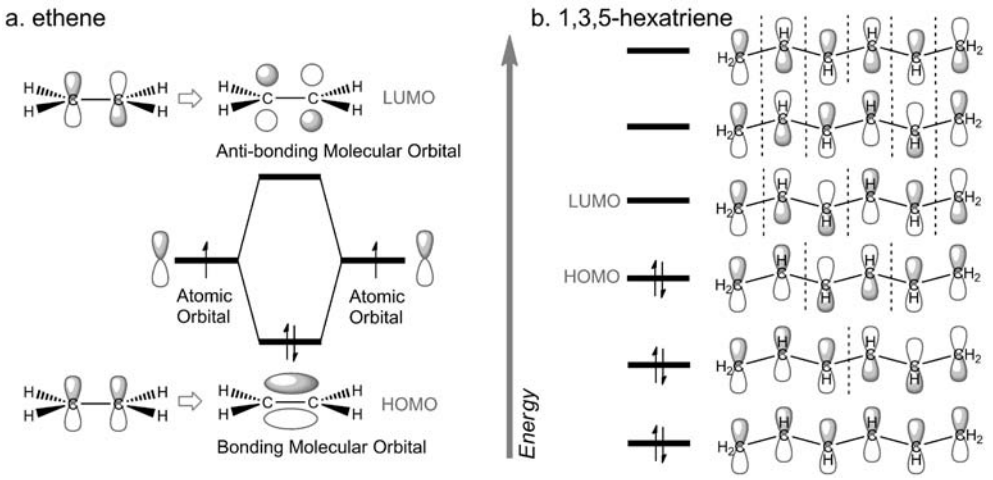

Figure 1.2 a. p_z-Orbitals of ethene and their combination into molecular orbitals, with the corresponding energy diagram. **b.** p_z-Orbitals of 1,3,5-hexatriene.

The more p_z-orbitals are present in the conjugated system, the more molecular orbitals are formed and the closer the spacing in energy between these orbitals, as is illustrated with 1,3,5-hexatriene in Figure 1.2b. Therefore, larger conjugated systems, in general, have a smaller HOMO-LUMO gap. This facilitates the introduction of charges (either positive or negative, due to oxidation or reduction of the molecule), which makes conjugated organic materials suitable for applications in electronics.

In 1977 Shirakawa, MacDiarmid, and Heeger found the conductivity of films of *trans*-polyacetylene to increase over seven orders of magnitude upon treatment with iodine vapor,[4] for which they were awarded with the Nobel prize in 2000. Iodine oxidizes polyacetylene and thus introduces positive charges (*i.e.*, doping), which are stabilized with I_3^- counter ions. Alternatively, charges can be introduced by an electric field, for instance when these polymers are used as the semiconductor in field-effect transistors (FET), or by light in organic photovoltaics (solar cells). Due to resonance structures (valence bond theory) or delocalized orbitals (molecular orbital theory) the charges are mobile within the π-conjugated

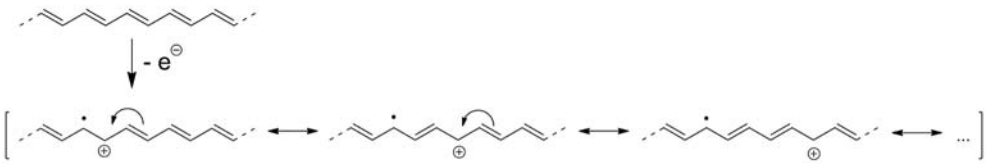

Figure 1.3 Charges that are introduced in a π-conjugated polymer chain are mobile, as represented by resonance structures.

polymer chains (Figure 1.3). Furthermore, they can 'hop' from one chain to the other (or from one part of a chain to another part of this chain), which makes conjugated polymers conductive materials.

1.3 Opportunities of π-Conjugation Topologies

1.3.1 Cross-conjugation

In the previous section we have discussed the properties of molecules with a framework of sp^2 hybridized carbon atoms. The strict pattern of alternating single and double bonds is called "linear conjugation" or "through conjugation". An alternative conjugation pattern is cross-conjugation, which is defined as "three unsaturated groups, two of which although conjugated to a third unsaturated center are not conjugated to each other".[5] In Figure 1.4a the pathway between **A** and **C** is linear conjugated, just as the pathway between **B** and **C**, whereas the pathway between **A** and **B** is cross-conjugated. Because all sp^2 hybridized carbon atoms in this structure have a perpendicular p_z-orbital and there is overlap between these p_z-orbitals, cross-conjugated molecules do show delocalization of electron density, although less than linear conjugated molecules.

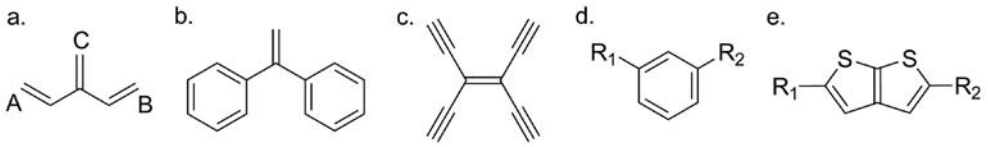

Figure 1.4 Examples of cross-conjugated molecules and building blocks.

Cross-conjugation originating from methylene side groups (Figure 1.4a and b) or substituted alkenes (Figure 1.4c) was reviewed by Tykwinsky.[6] We should note that also *meta*-substituted phenylenes (Figure 1.4d) are cross-conjugated. Cross-conjugated building-blocks as the thienothiophene in Figure 1.4e have been integrated in polymers and used in field-effect transistors, resulting in an improved air-stability and good mobility.[7] Very recently, cross-conjugated molecules have started to draw a lot of attention in the molecular electronics community due to

calculated quantum interference effects. This quantum interference effect lowers the molecular conductance at low bias voltages significantly,[8] as we will discuss in Chapter 5.

1.3.2 Omniconjugation

To realize electronic circuits of molecules only, π-conjugated molecules are the best candidates due to their conducting properties (Section 1.2). However, charge transport through these circuits should be *through* these molecular wires (for instance in the way that the carbocation "moves" through the chain in Figure 1.3) and not by hopping. Therefore we need linear conjugated pathways. A common method to design circuits of conjugated molecules is by interconnecting different parts via substituted benzene rings.[9-11] However, as we mentioned in the previous sections, the used *meta*-substitution of phenyl rings results in cross-conjugated pathways between the different parts of these molecules. Marleen van der Veen, a member of our group, has designed a more feasible alternative, so-called omniconjugated structures: "Omniconjugation is defined as the property of molecules, having direct linear π-conjugated pathways between *all* connected moieties."[12] Examples of omniconjugated structures are given in Figure 1.5.

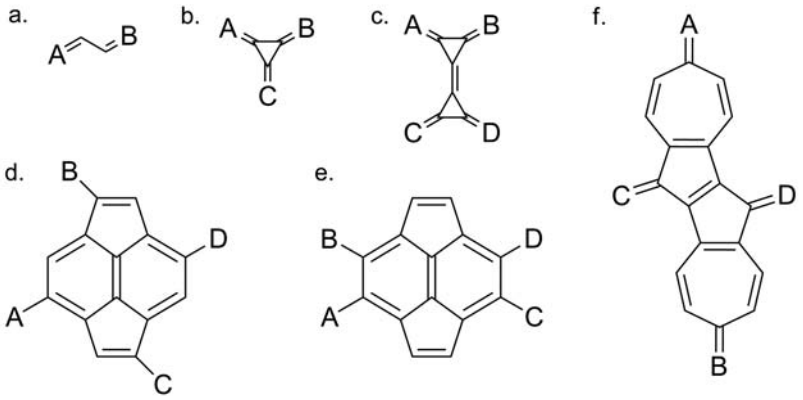

Figure 1.5 Examples of omniconjugated structures with two terminals (a), three terminals (b) and four terminals (c-f).

1.3.3 π-Logic

Omniconjugated molecules do not only have potential as interconnects in all-molecular electronic circuits, they can also be used to design molecules to perform logic operations. This concept was developed by Marleen van der Veen[13] and will be briefly explained in this section. Small circuits are used in current electronic devices to perform logic operations and it would be useful to replace these circuits by single elements. De Silva and co-workers came up with the idea to use molecules as logic elements.[14] They designed a molecular AND gate, in which ionic inputs determine the fluorescence output. Other molecular logic gates followed,[15] most of which yield optical signals as output. However, electrical outputs are desired for integration in solid-state devices. Rather complex examples are the OR and AND gates based on the molecular rectifier of Aviram and Ratner.[1,16]

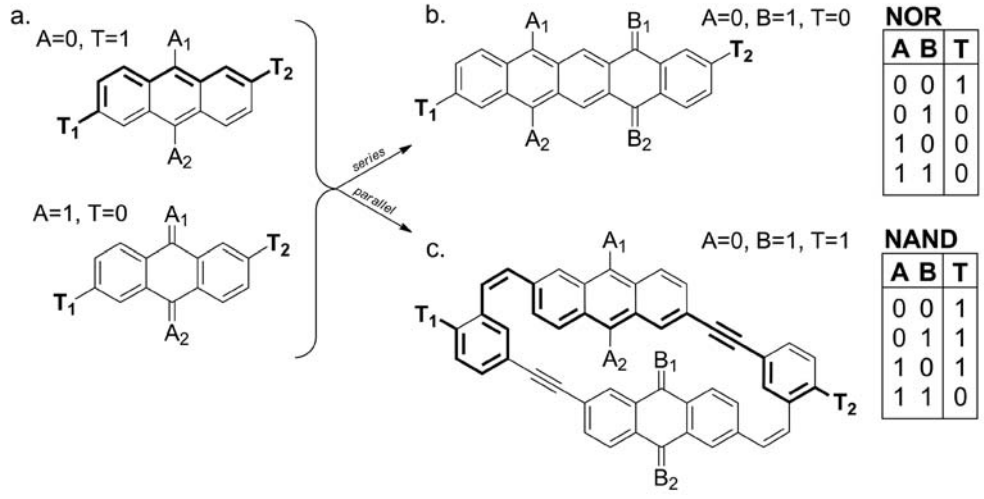

Figure 1.6 a. An example of a switch. Two of these switches can be combined in series (**b**) or parallel (**c**) to form logic NOR and NAND gates, of which the corresponding truth tables are shown.

Simple logic gates can be constructed from combinations of switches. The molecule in Figure 1.6a is an example of a switch: the pathway between T_1 and T_2 is linear conjugated (bold, defined as "*on*" or "1") when input channel A is connected via single bonds. Upon oxidation of the molecule (or passage of a soliton from A_1 to A_2, which converts all single bonds into double bonds and *vice versa*), A_1 and A_2 become connected via double bounds and the pathway from terminal T_1 to T_2 becomes cross-conjugated ("off" or "0"). Two of these switches

can be combined, which gives two input channels (A and B), each of which can be either connected by exocyclic single bonds (0) or by exocyclic double bonds (1). This gives four possibilities. Depending on the connection of the two switches, either in series (Figure 1.6b) or in parallel (Figure 1.6c), a logic NOR gate or a logic NAND gate is obtained.

This method of connecting switches only allows the design of a limited set of logic gates. Multiple NAND gates can in principle be connected in such a way that more complex logic gates like XOR and XNOR gates are obtained. Unfortunately, this leads again to rather large and unrealistic designs. A more elegant approach is the use of omniconjugated molecules to construct Boolean logic gates. The pyracylene compounds as drawn in Figure 1.5d and e are good candidates to be functionalized with additional terminals. Proper positioning of the two input channels (A_1-A_2 and B_1-B_2) and the read-out channel (T_1-T_2) allows the construction of 15 out of 16 Boolean logic gates.[13] Examples of a NAND-gate (more compact than the one in Figure 1.6c) and a XOR-gate, which is in general hard to design, are given in Figure 1.7.

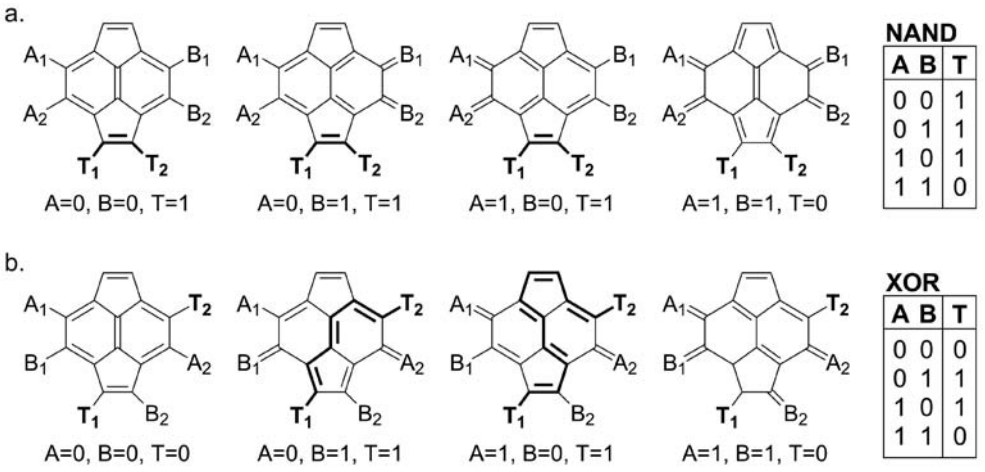

Figure 1.7 The four different states of a NAND gate (**a.**) and a XOR gate (**b.**), based on pyracylene molecules.

This concept of using relatively compact conjugated molecules with six terminals to perform logic operation is called "π-logic".[13] One of the main assumptions of this concept is that the conductance through linear conjugated pathways and cross-conjugated pathways is different. Linear conjugated pathways are expected to have a higher conductance ("1") than cross-conjugated pathways ("0"). The main

objective of this thesis is to find convincing evidence for this assumption by means of conductance measurements. This would establish this switching principle as the fundament for fast and efficient molecular logic operations.

1.4 Methods for Conductance Measurements

Before we can use molecules as components of electronic circuits,[17 - 21] we have to learn how single molecules or a single layer of molecules (*i.e.*, a self-assembled monolayer, SAM) behave electrically. In other words: we need to measure the current through the molecules upon applying a voltage. For that, we have to connect the molecule to (at least) two electrodes. Many methods have been developed to contact molecules, as reviewed by several groups.[22 - 27] We will describe a few techniques for conductance measurements of conjugated (di)thiols in the following section, not aiming at giving an elaborate overview of all possible techniques. Instead, we will mainly focus on the techniques we have been involved with *via* collaborations and to which we will return later in this thesis. Theoretical descriptions of charge transport through molecular junctions can be found in several reviews.[28 - 31]

1.4.1 Mechanically Controllable Break Junctions

A mechanically controllable break junction (MCBJ) consists of two sharp electrodes whose spacing can be adjusted and over which a voltage can be applied (Figure 1.8). The first MCBJ was prepared from a very thin metal wire that was glued to a flexible substrate.[32] A piezo element and two counter supports enabled controllable bending of the substrate. The wire was deeply notched and bending of the substrate caused a fracture in the wire. In 1997 Reed *et al.* reported on the conductance of benzenedithiol, using a similar setup.[33] They placed a glass tube on the junction and filled this with a mM solution of 1,4-benzenedithiol in THF, to form a SAM of these molecules on the gold wire. They broke the wire by bending the substrate and brought the electrodes together until a spacing of about 8 Å (the calculated length of the dithiol). In this position a voltage was applied and current-voltage (*I-V*) measurements were performed, from which was concluded that a single molecule or a few molecules were measured.

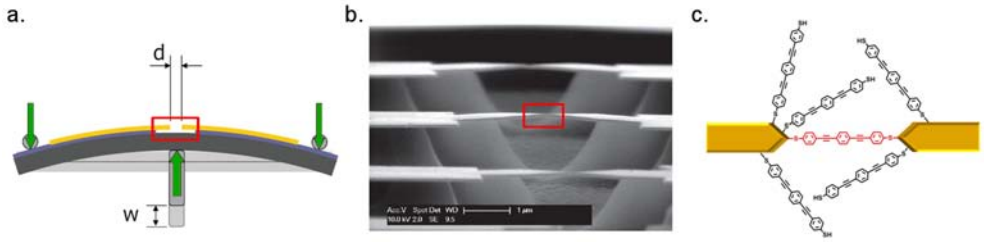

Figure 1.8 a. Schematic of a lithographically defined mechanically controllable break junction in which the displacement of the pushing rod (w) defines the spacing between the electrodes (d). **b.** Scanning electron microscopy image of the suspended gold bridge of three lithographically defined break junctions in parallel. **c.** Schematic of a conjugated molecule in a break junction.

Van Ruitenbeek *et al.* succeeded in downscaling the device dimensions by two orders of magnitude.[34] They prepared break junctions using electron beam lithography on a bendable phosphor-bronze substrate, which resulted in devices with a free hanging metal bridge of about 2 μm (Figure 1.8b). When such a lithographically defined junction is broken, two atomically sharp nanometer-wide electrodes are formed. MCBJs can be operated either in a liquid environment[35] or in UHV and at low temperatures (4.2 K).[36] This results in highly stable junctions[37] with control over the spacing between the electrodes. Several conjugated molecules have been studied in MCBJs by recording *I-V* curves.[38-41] However, since the shape of the gold electrode and the binding of the molecules vary from junction to junction, statistical approaches have been introduced to increase the reproducibility of the measurements.[42-44]

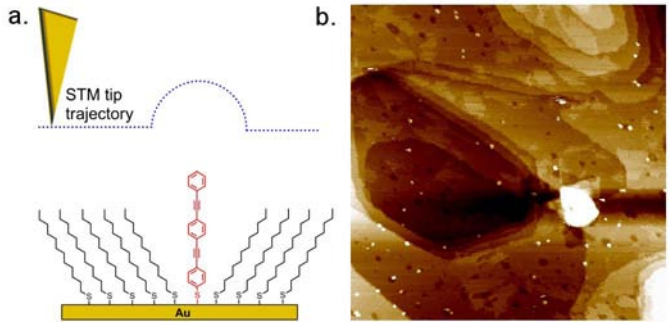

Figure 1.9 a. Schematic of the STM tip trajectory when imaging a mixed SAM at constant current mode. **b.** STM image of a mixed SAM of OPE3 and dodecanethiol on gold (180x180 nm, height scale is 25 Å). This image shows the terraces of the gold surface, two differently packed phases of dodecanethiol molecules (small difference in contrast) and bundles of OPE3 molecules as white spots.

1.4.2 Scanning Tunneling Microscopy

The first Scanning Tunneling Microscope (STM) was built by Binnig and Ruhrer from IBM Zürich in 1981, for which they were awarded with the Nobel Prize in Physics in 1986. A metal tip is brought in close proximity to a conducting surface and a bias voltage is applied between the tip and the surface. A STM can be operated at constant current mode, in which the height of the tip is adjusted by a feedback loop in such a way that the current remains constant when a surface is scanned (line by line), which results in an image of the surface.[45] Molecular resolution is easily achieved nowadays.

The conductance of conjugated molecules has been studied by STM via different approaches. An approach that was first reported in 1996 is STM imaging of mixed SAMs.[46] First a SAM of alkanethiol molecules is grown on a gold surface. Conjugated thiols (or dithiols) are subsequently inserted by immersion of the alkanethiol SAM in a solution with a low concentration of these conjugated molecules. Since the conductance of these molecules is higher than that of the surrounding alkanethiol molecules, the tip has to move up (and increase the gap between tip and SAM) to retain the tunneling current constant (Figure 1.9a). The conjugated molecules appear in the STM image as light spots (Figure 1.9b). The "apparent height"[47] of these spots is a measure for the conductance of the conjugated molecules.[48 - 52] Disadvantages of these method are that the formation of mixed SAMs is not trivial and that conjugated thiols tend to insert at defects[53] or as bundles of molecules (as is the case in Figure 1.9). Furthermore, the apparent height could depend on the packing of the surrounding alkanethiol molecules, on the binding of the conjugated thiol to the gold surface, on the imaging parameters, and on the shape and cleanliness of the tip, which obfuscates the comparison of images. Changes in the binding of the conjugated thiol to the gold surface have been observed as "stochastic switching".[54-56] An approach to overcome these problems is to study *in situ* switching of the molecules by external stimuli as light[57] or electrochemical potential.[58]

Recording *I-V* curves at specific spots above a SAM (often combined with imaging) is an alternative approach on molecular conductance.[59] A disadvantage is the presence of an unknown air (or vacuum) gap between the molecule and the tip.

A third approach to study the conductance of single molecules with an STM setup is the STM break junction approach as introduced by Tao in 2003.[60] An STM tip is

brought close to the SAM, after which the feedback of the STM is turned off. The STM tip is then pushed into the substrate and subsequently retracted, while the current is recorded (Figure 2.1). This results in the formation of molecular junctions, similar to those by the MCBJ technique as described in the previous section. An advantage is the speed of a STM setup, which allows the collection of thousands of curves (required for a histogram) in a few hours. Instead of pushing the STM tip into the surface, a soft contact approach can be used, in which the tip only gently touches the SAM and not the underlying metal surface[61] or the tip can be placed at different distances from the surface and the current can be recorded, while waiting for a junction to form.[62] The STM break junction approach is generally applied in a liquid environment and can be combined with *in situ* electrochemistry.[63] More details on STM break junction measurements are given in Chapter 4.

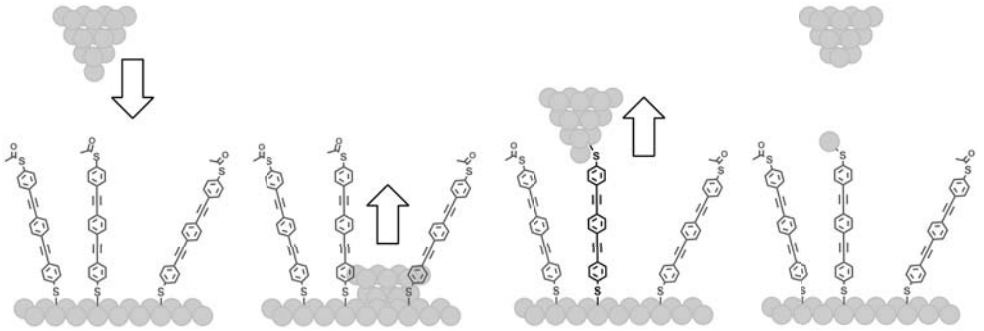

Figure 1.10 Schematic of the STM break junction approach, in which the STM tip is brought into contact with the gold substrate and then withdrawn.

1.4.3 Conductive Probe Atomic Force Microscopy

Another scanning probe method that is frequently used to study molecular conductance is conductive probe atomic force microscopy (CP-AFM). Where in STM imaging a gap between the tip and the monolayer is present, CP-AFM is used in contact mode. The use of a conductive tip (for instance coated with gold) allows to measure the current between the tip and the sample on a specific spot on the surface. Single conjugated molecules (or bundles of these molecules) can be studied when first a mixed SAM is formed with conjugated dithiols inserted in a SAM of alkanemonothiols.[64-66] Subsequently this mixed SAM is immersed in a

solution of gold nanoparticles, which bind on the free thiol groups of the inserted conjugated molecules (Figure 1.11a). These gold nanoparticles can be observed in an AFM image and then be contacted with the CP-AFM tip, which makes it possible to measure *I-V* curves on the single (bundle of) molecule(s). Mixed SAMs coated with gold nanoparticles have also been investigated by STM.[67]

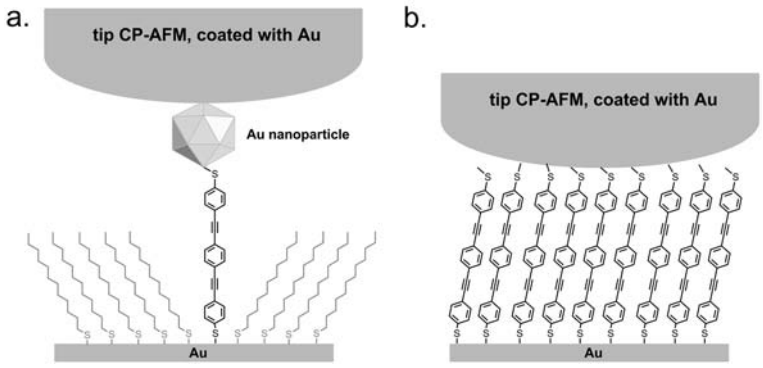

Figure 1.11 a. Schematic of a gold coated AFM that contacts a gold nanoparticle on a conjugated molecule, which is inserted in an alkanethiol SAM. **b.** Schematic of a gold coated AFM tip which directly contacts a SAM of conjugated molecules.

A more straightforward approach is to directly contact a densely-packed SAM of conjugated molecules with a gold-coated AFM tip and measure the *I-V* characteristics of the SAM (Figure 1.11b).[68] This method is developed and described in detail by Frisbie's group.[69] We estimate that the number of molecules that are contacted this way is in the order of hundreds.

1.4.4 Liquid Metal Junctions

One of the challenges of contacting a SAM over a larger area to measure its conductance is to make a decent contact without damaging the SAM. Liquid metals are good candidates to form the such a top contact. Mercury has been used in several groups for this purpose.[70-73] A disadvantage of mercury is that it only forms stable contacts when surrounded by an alkanethiol SAM and in a liquid environment. When a SAM of conjugated thiols is the object of study, a tunneling current is measured from the metal substrate through the conjugated thiol and the alkanethiol to the mercury, thus through two monolayers.

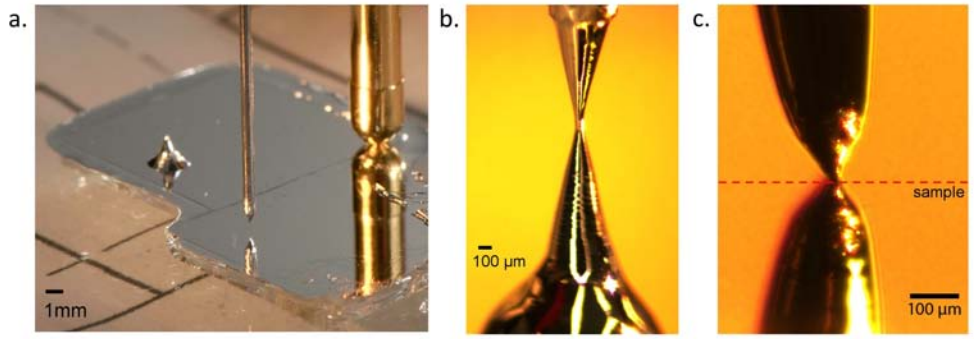

Figure 1.12 a. Photo of a sample in the EGaIn setup, showing the syringe needle with the EGaIn tip in the middle of the photo. **b.** Microscope image of the formation of the EGaIn tip by withdrawal of the syringe from a sacrificial drop of EGaIn. **c.** Microscope image of an EGaIn tip contacting a surface (including the reflection of the tip by the surface).

An alternative liquid metal is the eutectic alloy of gallium (75%) and indium (25%), abbreviated as EGaIn, with a melting point of 15.5°C.[74] Though EGaIn is a liquid, the thin shell of gallium oxide (~1 nm) makes that it does not necessarily has a drop shape, instead conical tips can be formed (Figure 1.12). This allows its use to contact SAMs in ambient conditions and to measure the I-V characteristics of the SAM.[75,76] The contact area of such a tip is in the order of 10-100 µm and is measured for each junction with a high magnification camera.

1.4.5 Large Area Molecular Junctions

The aforementioned techniques all have control over the distance of at least one of the two electrodes, which allows the formation and breaking of the junction. The fabrication of Large Area Molecular Junction (LAMJ) devices[77] is irreversible,

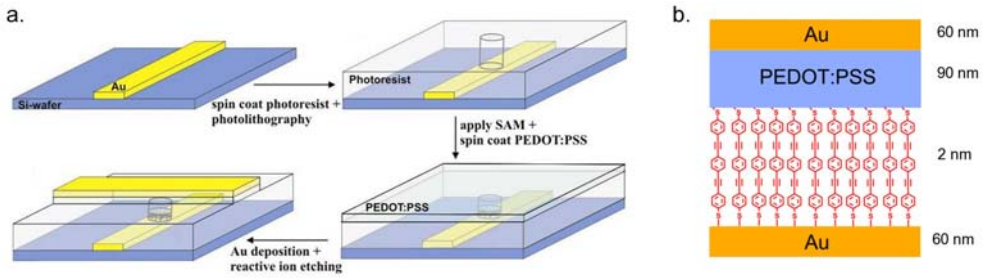

Figure 1.13 a. Schematic of the fabrication procedure of LAMJs, starting with the evaporation of the bottom contact on a silicon wafer, followed by lithographical definition of pores in a photoresist layer. After cleaning the gold, SAMs are grown inside these pores. Then PEDOT:PSS is spin coated on the wafer and the gold top contact is evaporated, after which the excess of PEDOT:PSS that is not covered by the gold top contact is removed (adopted from ref. 77). **b.** Schematic of the junction.

since the SAM is sandwiched between two solid electrodes. Earlier attempts to form this type of solid junctions by evaporation of a metal top contact on a SAM (that was grown on a bottom contact) resulted in shorts due to penetration of the metal through the SAM,[78,79] which limited the junction size[80] and the yield of non-shorted devices.[81] These problems were overcome by spin coating a layer of metallic conducting polymer on top of the SAM before evaporation of the a top contact (see Figure 1.13).[77,82] The water-based suspension of heavily oxidized poly(3,4-ethylene-dioxythiophene) stabilized with poly(4-styrenesulfonate) counterions (PEDOT:PSS) is mainly used for this purpose. This trick allows the formation of stable junctions[83] up to 100 μm in diameter in over 95% yield.[77] Further development of the fabrication process resulted in wafers with over 20000 junctions and in series connection of up to 200 junctions.[84]

1.4.6 Arrays of Gold Nanoparticles

As alternative to repetitive formation and breaking of single molecular junctions to obtain statistical data on molecular conductance, arrays of gold nanoparticles were developed to measure many junctions (both in series and parallel) simultaneously and obtain average conductances (or resistances) for gold-molecule-gold junctions that way.[85] First gold nanoparticles are synthesized, covered with octanethiol molecules, and dissolved in chloroform. A drop of this solution is placed at an air-water interface, where the gold nanoparticles self-assemble into a 2D array (Figure 1.14). This array is transferred onto a substrate using a patterned PDMS stamp and gold contacts are evaporated. The sheet resistance of the array between these contacts is measured.

The array can be immersed in a solution of dithiols (for example conjugated OPE3), that exchange with some of the octanethiol molecules. Since these OPE3 dithiols can bind to two adjacent nanoparticles (and are conjugated), the resistance of the networks drops with a factor 100-1000 to about the resistance of a single OPE3 molecular junction. Exchange with OPE3 monothiol molecules lowers the resistance of the network, though less than OPE3 dithiol molecules.[86] The exchange process has been confirmed by the reversible shift of the UV-Vis absorption from the surface plasmon resonance of the gold nanoparticles, and reversible changes in the IR spectra of the networks.[87] Different conjugated dithiols can be inserted in the array via exchange processes and the resulting resistances can be compared. Alternatively, the inserted molecules can be switched by external

stimuli (*i.e.*, light or redox chemistry) and this switching process can be monitored by measuring changes in the resistance.[88,89]

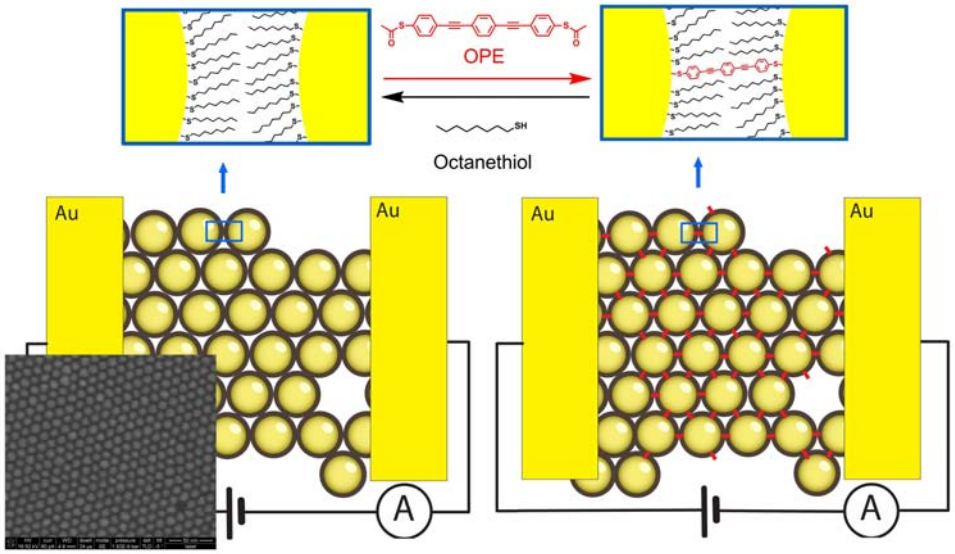

Figure 1.14 Schematic of a 2D array of octanethiol-covered gold nanoparticles through which the current is measured. Octanethiol molecules (black) can be reversibly exchanged by dithiolated OPE3 molecules (red), which reduces the resistance of the network by two to three orders of magnitude. The inset shows a scanning electron microscopy image of a 2D array of octanethiol-covered gold nanoparticles transferred onto a silicon wafer.

1.5 Our Matrix Approach

In Section 1.3 we have discussed the concept of using π-conjugated molecules as logic gates.[13] To study this π-logic proposal experimentally, techniques by which at least three (preferably four) terminals can be contacted are required. In known three-terminal junctions the third electrode is a gate, which does not directly contact the molecule(s) as the other electrodes do.[90,91] The π-logic idea is based on conductance differences between linear conjugated and cross-conjugated pathways between terminals. The main aim of this thesis is therefore to study this difference experimentally.

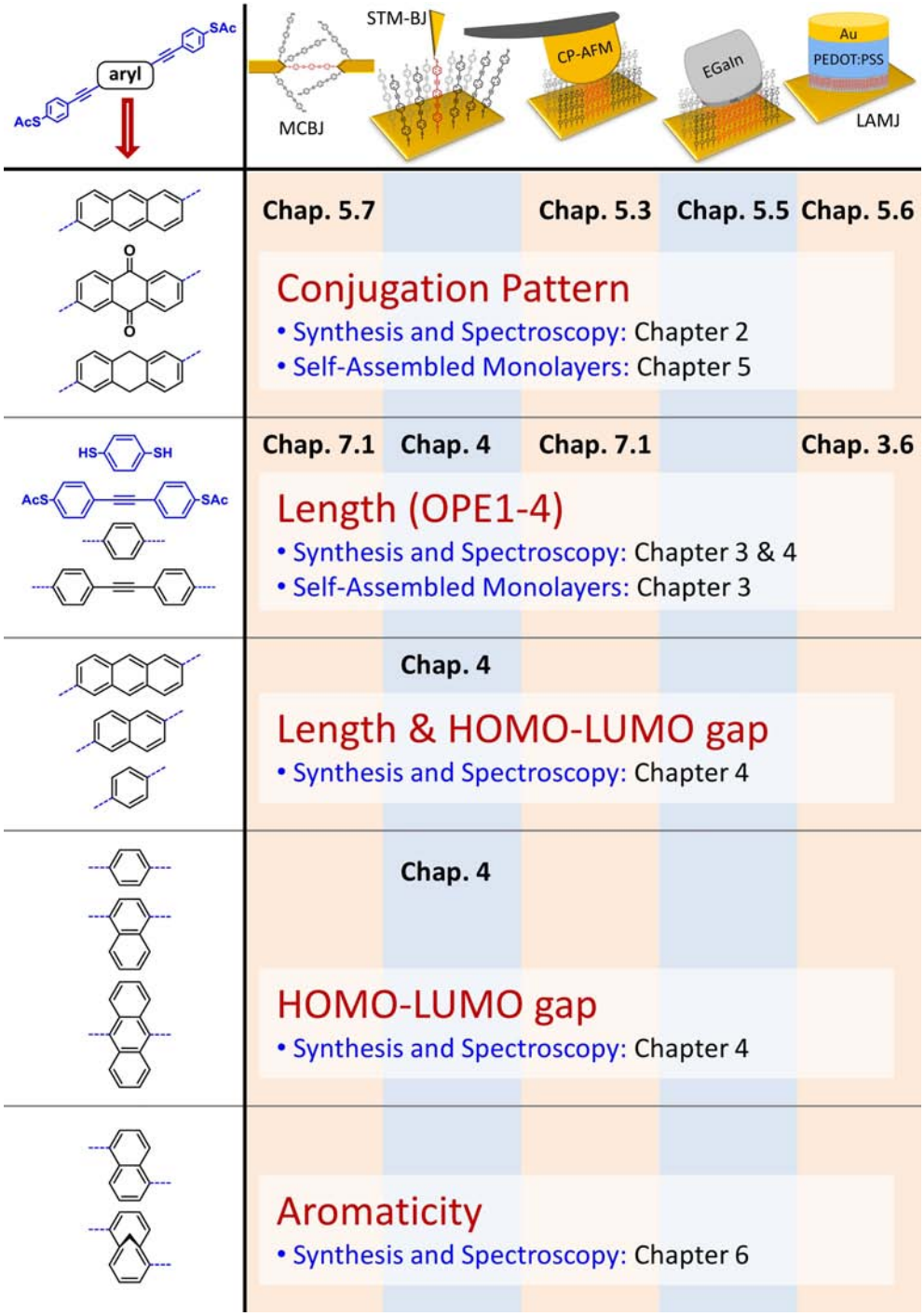

Figure 1.15 The Matrix Approach, in which we study the conductance of five series of molecules (left) by various methods (top). The series of molecules are constructed by varying the central unit.

We have developed an anthraquinone-based switch derived from the structure in Figure 1.6a.[92] This cross-conjugated anthraquinone-based switch becomes linear conjugated upon (electro)chemical reduction, in solution. In Chapter 2 we describe the synthesis and spectroscopic properties of this cross-conjugated state of the switch and several reference compounds that are linear conjugated or have a broken conjugation pattern. Since the conductance measurements on a single, switching molecule inside a junction under electrochemical control were found to be non-trivial, we have broadened our scope, aiming at measuring reliable conductance data on conjugated molecules. For that, we developed several series of conjugated molecules, which allow to study trends in the relation between molecular structure and conductance. All the molecules have oligo(phenylene ethynylene) (OPE) based structures, of which we either substitute the core phenylene with any aryl group (as drawn in the left column of Figure 1.15) or vary the length (second series in Figure 1.15). Though phenylene enthynylene based oligomers and polymers[93] are not as widely used in organic electronics[94] as for instance the phenylene vinylenes (OPVs and PPVs), OPE-type molecules are present in molecular electronics from the early days.[95,96] Advantages of OPE-type molecules are their rigidity and linearity, which limits the conformational freedom and therefore rules out one source of variety in conductance measurements. We use acetyl-protected thiol anchoring groups for all molecular wires.

We study the conductance of these series of molecular wires by several methods (Section 1.4), ranging from single molecule measurements (MCBJ and STM-BJ), to measurements on hundreds of molecules (CP-AFM) and areas up to 8000 μm^2 (corresponding to ~$3x10^{10}$ molecules[97]; EGaIn and LAMJ). This study of five series by five methods constitutes our "Matrix Approach" (Figure 1.15). The comparison of data from different measurements allows to distinguish trends caused by the molecular structure and technique dependent trends. All conductance measurements were performed in collaborations with:

- Veerabhadrarao Kaliginedi, Wenjing Hong, Pavel Moreno García, and prof. Thomas Wandlowski, University of Bern (STM-BJ and ambient MCBJ)
- Constant Guédon and Sense Jan van der Molen, Leiden University (CP-AFM and arrays of gold nanoparticles)
- Eek Huisman, Auke Kronemeijer, Ilias Katsouras, Paul van Hal, Tom

Geuns, and prof. Dago de Leeuw, University of Groningen and Philips Research Eindhoven (LAMJ)

- Davide Fracasso and Ryan Chiechi, University of Groningen (EGaIn)
- Christian Martin, Roel Smit, Diana Dulić, Mickael Perrin, Ferry Prins, Jos Seldenthuis, prof. Herre van der Zant, and prof. Jan van Ruitenbeek, Delft University of Technology and Leiden University (UHV and low temperature MCBJ)
- Víctor García-Suárez and prof. Colin Lambert, Lancaster University (calculations)
- Troels Markussen and prof. Kristian Thygesen, Technical University of Denmark (calculations)

In Chapter 3 we describe how high quality, densely packed self-assembled monolayers of π-conjugated dithiols can be formed, because this is required for reliable measurements by LAMJ, EGaIn and CP-AFM. Furthermore, we will demonstrate the influence of the conditions used for the formation of self-assembled monolayers of OPEs on the resistance by LAMJ. In Chapter 4 we describe the trends found in STM-BJ measurements on three of the five series. Chapter 5 discusses the influence of conjugation patterns on the molecular conductance, as studied by various methods. In Chapter 6 we focus on the synthesis of methano[10]annulene-based molecular wires and polymers. We return to the Matrix Approach in Chapter 7 by summarizing all results, discussing additional results and comparing techniques, to find the main conclusions of this thesis.

1.6 References and Notes

1. A. Aviram, M.A. Ratner, *Chem. Phys. Lett.* **1974**, *29*, 277-283.
2. The history of Molecular Electronics is described in: N.S. Hush, *Ann. NY Acad. Sci.* **2003**, *1006*, 1-20.
3. C. Joachim, J.K. Gimzewski, A. Aviram, *Nature* **2000**, *408*, 541-548.
4. H. Shirakawa, E.J. Louis, A.G. MacDiarmid, C.K. Chiang, A.J. Heeger, *J. Chem. Soc., Chem. Commun.* **1977**, 578-580.
5. N.F. Phelan, M. Orchin, *J. Chem. Educ.* **1968**, *45*, 633.
6. M. Gholami, R.R. Tykwinski, *Chem. Rev.* **2006**, *106*, 4997-5027.
7. M. Heeney, C. Bailey, K. Genevicius, M. Shkunov, D. Sparrowe, S. Tierney, I. McCulloch, *J. Am. Chem. Soc.* **2005**, *127*, 1078-1079; I. McCulloch, M. Heeney, M.L. Chabinyc, D. DeLongchamp, R.J. Kline, M. Cölle, W. Duffy, D. Fischer, D. Gundlach, B. Hamadani, R. Hamilton, L. Richter, A. Salleo, M. Shkunov, D. Sparrowe, S. Tierney, W. Zhang, *Adv. Mater.* **2009**, *21*, 1091-1109.
8. G.C. Solomon, D.Q. Andrews, R.H. Goldsmith, T. Hansen, M.R. Wasielewski, R.P. Van Duyne, M.A. Ratner, *J. Am. Chem. Soc.* **2008**, *130*, 17301-17308; D.Q. Andrews, G.C. Solomon, R.H. Goldsmith, T. Hansen, M.R. Wasielewski, R.P. Van Duyne, M.A. Ratner, *J. Phys. Chem. C* **2008**, *112*, 16991-16998.
9. J.M. Tour, M. Kozaki, J.M. Seminario, *J. Am. Chem. Soc.* **1998**, *120*, 8486-8493.
10. J.C. Ellenbogen, J.C. Love, *Proc. IEEE* **2000**, *88*, 386-426.
11. N. Zhou, L. Wang, D.W. Thompson, Y. Zhao, *Org. Lett.* **2008**, *10*, 3001-3004.
12. M.H. van der Veen, M.T. Rispens, H.T. Jonkman, J.C. Hummelen, *Adv. Funct. Mater.* **2004**, *14*, 215-223; M.H. van der Veen, H.T. Jonkman, J.C. Hummelen, *AIP Conf. Proc.* **2004**, *723*, 321-325.
13. M.H. van der Veen, *PhD Thesis* "π-Logic" *University of Groningen*, **2006**.
14. P.A. de Silva, N.H.Q. Gunaratne, C.P. McCoy, *Nature* **1993**, *364*, 42-44.
15. V. Balzani, A. Credi, M. Venturi, *ChemPhysChem* **2003**, *3*, 49-59.
16. S. Ami, M. Hliwa, C. Joachim, *Chem.Phys.Lett.* **2003**, *367*, 662-668.
17. F.L. Carter, *J. Vac. Sci. Technol., B* **1983**, *1*, 959-968; F. Carter, *Phys. D* **1984**, *10*, 175-194.
18. N.J. Tao, *Nat. Nanotechnol.* **2006**, *1*, 173-181.
19. N. Weibel, S. Grunder, M. Mayor, *Org. Biomol. Chem.* **2007**, *5*, 2343-2353.
20. R.L. McCreery, A.J. Bergren, *Adv. Mater.* **2009**, *21*, 4303-4322.
21. S.J. van der Molen, P. Liljeroth, *J. Phys.: Condens. Matter* **2010**, *22*, 133001.
22. D.L. Allara, T.D. Dunbar, P.S. Weiss, L.A. Bumm, M.T. Cygan, J.M. Tour, W.A. Reinerth, Y. Yao, M. Kozaki, L. Jones II, *Ann. NY Acad. Sci.* **1998**, *852*, 349-370.
23. B.A. Mantooth, P.S. Weiss, *Proc. IEEE* **2003**, *9*, 1785-1802.
24. H.B. Akkerman, B. de Boer, *J. Phys.: Condens. Matter* **2008**, *20*, 013001.
25. H. Haick, D. Cahen, *Prog. Surf. Sci.* **2008**, *83*, 217-261.

26. N. Prokopuk, K. Son, *J. Phys.: Condens. Matter* **2008**, *20*, 374116.

27. T. Li, W. Hu, D. Zhu, *Adv. Mater.* **2010**, *22*, 286-300.

28. A. Salomon, D. Cahen, S. Lindsay, J. Tomfohr, V.B. Engelkes, C.D. Frisbie, *Adv. Mater.* **2003**, *15*, 1881-1890.

29. S.M. Lindsay, M.A. Ratner, *Adv. Mater.* **2007**, *19*, 23-31.

30. J.M. Thijssen, H.S.J. van der Zant, *Phys. Status Solidi B* **2008**, *245*, 1455-1470.

31. R.M. Metzger, *J. Mater. Chem.* **2008**, *18*, 4364-4396.

32. C.J. Muller, J.M. van Ruitenbeek, L.J. de Jongh, *Phys. C* **1992**, *191*, 485-504.

33. M.A. Reed, C. Zhou, C.J. Muller, T.P. Burgin, J.M. Tour, *Science* **1997**, *278*, 252-254.

34. J.M. van Ruitenbeek, A. Alvarez, I. Pineyro, C. Grahmann, P. Joyez, M.H. Devoret, D. Esteve, C. Urbina, *Rev. Sci. Instrum.* **1996**, *67*, 108-111.

35. L. Grüter, M.T. González, R. Huber, M. Calame, C. Schönenberger, *Small* **2005**, *1*, 1067-1070.

36. R.H.M. Smit, Y. Noat, C. Untiedt, N.D. Lang, M.C. van Hemert, J.M. van Ruitenbeek, *Nature* **2002**, *419*, 906-909.

37. M.L. Trouwborst, E.H. Huisman, F.L. Bakker, S.J. van der Molen, B.J. van Wees, *Phys. Rev. Lett.* **2008**, *100*, 175502.

38. C. Kergueris, J.-P. Bourgoin, S. Palacin, D. Esteve, C. Urbina, M. Magoga, C. Joachim, *Phys. Rev. B* **1999**, *59*, 12505-12513.

39. M. Mayor, C. von Hänisch, H.B. Weber, J. Reichert, D. Beckmann, *Angew. Chem., Int. Ed.* **2002**, *41*, 1183-1186; J. Reichert, R. Ochs, D. Beckmann, H.B. Weber, M. Mayor, H.v. Löhneysen, *Phys. Rev. Lett.* **2002**, *88*, 176804; M. Mayor, H.B. Weber, J. Reichert, M. Elbing, C. von Hänisch, D. Beckmann, M. Fischer, *Angew. Chem., Int. Ed.* **2003**, *42*, 5834-5838.

40. E. Lörtscher, J.W. Ciszek, J. Tour, H. Riel, *Small* **2006**, *2*, 973-977; E. Lörtscher, M. Elbing, M. Tschudy, C. von Hänisch, H.B. Weber, M. Mayor, H. Riel, *ChemPhysChem* **2008**, *9*, 2252-2258.

41. D. Dulić, S.J. van der Molen, T. Kudernac, H.T. Jonkman, J.J.D. de Jong, T.N. Bowden, J. van Esch, B.L. Feringa, B.J. van Wees, *Phys. Rev. Lett.* **2003**, *91*, 207402.

42. M.T. González, S. Wu, R. Huber, S.J. van der Molen, C. Schönenberger, M. Calame, *Nano Lett.* **2006**, *6*, 2238-2242.

43. E. Lörtscher, H.B. Weber, H. Riel, *Phys. Rev. Lett.* **2007**, *98*, 176807.

44. C.A. Martin, D. Ding, J.K. Sørensen, T. Bjørnholm, J.M. van Ruitenbeek, H.S.J. van der Zant, *J. Am. Chem. Soc.* **2008**, *130*, 13198-13199.

45. E. Meyer, H.J. Hug, R. Bennewitz, *Scanning Probe Microscopy: The Lab on a Tip*, Springer **2004**.

46. L.A. Bumm, J.J. Arnold, M.T. Cygan, T.D. Dunbar, T.P. Burgin, L. Jones II, D.L. Allara, J.M. Tour, P.S. Weiss, *Science* **1996**, *271*, 1705-1707.

47. L.A. Bumm, J.J. Arnold, T.D. Dunbar, D.L. Allara, P.S. Weiss, *J. Phys. Chem. B* **1999**, *103*, 8122-8127.

48. L. Patrone, S. Palacin, J.P. Bourgoin, J. Lagoute, T. Zambelli, S. Gauthier, *Chem. Phys.* **2002**, *281*, 325-332.

49. P.A. Lewis, C.E. Inman, F. Maya, J.M. Tour, J... Hutchison, P.S. Weiss, *J. Am. Chem. Soc.*

2005, *127*, 17421-17426.

50. A.M. Moore, A.A. Dameron, B.A. Mantooth, R.K. Smith, D.J. Fuchs, J.W. Ciszek, F. Maya, Y. Yao, J.M. Tour, P.S. Weiss, *J. Am. Chem. Soc.* **2006**, *128*, 1959-1967.
51. K. Moth-Poulsen, L. Patrone, N. Stuhr-Hansen, J.B. Christensen, J.-P. Bourgoin, T. Bjørnholm, *Nano Lett.* **2005**, *5*, 783-785.
52. K. Ishizuka, M. Suzuki, S. Fuji, U. Akiba, Y. Takayama, F. Sato, M. Fujihira, *Jpn. J. Appl. Phys.* **2005**, *44*, 5382-5385.
53. M.T. Cygan, T.D. Dunbar, J.J. Arnold, L.A. Bumm, N.F. Shedlock, T.P. Burgin, L. Jones II, D.L. Allara, J.M. Tour, P.S. Weiss, *J. Am. Chem. Soc.* **1998**, *120*, 2721-2732.
54. Z.J. Donhauser, B.A. Mantooth, T.P. Pearl, K.F. Kelly, S.U. Nanayakkara, P.S. Weiss, *Jpn. J. Appl. Phys.* **2002**, *41*, 4871-4877.
55. A. Hallbäck, B. Poelsema, H.J.W. Zandvliet, *ChemPhysChem* **2007**, *8*, 661-665.
56. A.M. Moore, B.A. Mantooth, Z.J. Donhauser, Y. Yao, J.M. Tour, P.S. Weiss, *J. Am. Chem. Soc.* **2007**, *129*, 10352-10353.
57. N. Katsonis, T. Kudernac, M. Walko, S.J. van der Molen, B.J. van Wees, B.L. Feringa, *Adv. Mater.* **2006**, *18*, 1397-1400; S.J. van der Molen, H. van der Vegte, T. Kudernac, I. Amin, B.L. Feringa, B.J. van Wees, *Nanotechnology* **2006**, *17*, 310-314.
58. S. Tsoi, I. Griva, S.A. Trammell, A.S. Blum, J.M. Schnur, N. Lebedev, *ACS Nano* **2008**, *2*, 1289-1295.
59. S. Hong, R. Reifenberger, W. Tian, S. Datta, J. Henderson, C.P. Kubiak, *Superlattices Microstruct.* **2000**, *28*, 289-303.
60. B. Xu, N.J. Tao, *Science* **2003**, *301*, 1221-1223.
61. C. Li, I. Pobelov, T. Wandlowski, A. Bagrets, A. Arnold, F. Evers, *J. Am. Chem. Soc.* **2008**, *130*, 318-326.
62. W. Haiss, R.J. Nichols, H. van Zalinge, S.J. Higgins, D. Bethell, D.J. Schiffrin, *Phys. Chem. Chem. Phys.* **2004**, *6*, 4330-4337; W. Haiss, C. Wang, I. Grace, A.S. Batsanov, D.J. Schiffrin, S.J. Higgins, M.R. Bryce, C.J. Lambert, R.J. Nichols, *Nat. Mater.* **2006**, *5*, 995-1002.
63. I.V. Pobelov, Z. Li, T. Wandlowski, *J. Am. Chem. Soc.* **2008**, *130*, 16045-16054.
64. X.D. Cui, A. Primak, X. Zarate, J. Tomfohr, O.F. Sankey, A.L. Moore, T.A. Moore, D. Gust, G. Harris, S.M. Lindsay, *Science* **2001**, *294*, 571-574.
65. G.K. Ramachandran, T.J. Hopson, A.M. Rawlett, L.A. Nagahara, A. Primak, S.M. Lindsay, *Science* **2003**, *300*, 1413-1416.
66. D.S. Seferos, A.S. Blum, J.G. Kushmerick, G.C. Bazan, *J. Am. Chem. Soc.* **2006**, *128*, 11260-11267.
67. A.S. Blum, J.C. Yang, R. Shashidhar, B. Ratna, *Appl. Phys. Lett.* **2003**, *82*, 3322-3324; A.S. Blum, J.G. Kushmerick, D.P. Long, C.H. Patterson, J.C. Yang, J.C. Henderson, Y. Yao, J.M. Tour, R. Shashidhar, B.R. Ratna, *Nat. Mater.* **2005**, *4*, 167-172.
68. D.J. Wold, C.D. Frisbie, *J. Am. Chem. Soc.* **2001**, *123*, 5549-5556.
69. V.B. Engelkes, J.M. Beebe, C.D. Frisbie, *J. Phys. Chem. B* **2005**, *109*, 16801-16810.
70. K. Slowinski, H.K.Y. Fong, M. Majda, *J. Am. Chem. Soc.* **1999**, *121*, 7257-7261; R.L. York, P.T. Nguyen, K. Slowinski, *J. Am. Chem. Soc.* **2003**, *125*, 5948-5953.
71. M.A. Rampi, G.M. Whitesides, *Chem. Phys.* **2002**, *281*, 373-391.

72. E.A. Weiss, R.C. Chiechi, G.K. Kaufman, J.K. Kriebel, Z. Li, M. Duati, M.A. Rampi, G.M. Whitesides, *J. Am. Chem. Soc.* **2007**, *129*, 4336-4349.

73. F.C. Simeone, M.A. Rampi, *Chimia* **2010**, *64*, 362-369.

74. S.J. French, D.J. Saunders, G.W. Ingle, *J. Phys. Chem.* **1938**, *42*, 265-274.

75. R.C. Chiechi, E.A. Weiss, M.D. Dickey, G.M. Whitesides, *Angew. Chem., Int. Ed.* **2008**, *47*, 142-144.

76. C.A. Nijhuis, W.F. Reus, G.M. Whitesides, *J. Am. Chem. Soc.* **2009**, *131*, 17814-17827.

77. H.B. Akkerman, P.W.M. Blom, D.M. de Leeuw, B. de Boer, *Nature* **2006**, *441*, 69-72.

78. B. de Boer, M.M. Frank, Y.J. Chabal, W. Jiang, E. Garfunkel, Z. Bao, *Langmuir* **2004**, *20*, 1539-1542.

79. H. Haick, J. Ghabboun, D. Cahen, *Appl. Phys. Lett.* **2005**, *86*, 042113.

80. W. Wang, T. Lee, M.A. Reed, *Phys. Rev. B* **2003**, *68*, 035416.

81. T.-W. Kim, G. Wang, H. Lee, T. Lee, Nanotechnology 2007, 18, 315204.

82. F. Milani, C. Grave, V. Ferri, P. Samorì, M.A. Rampi, *ChemPhysChem* **2007**, *8*, 515-518.

83. H.B. Akkerman, A.J. Kronemeijer, J. Harkema, P.A. van Hal, E.C.P. Smits, D.M. de Leeuw, P.W.M. Blom, *Org. Electron.* **2010**, *11*, 146-149.

84. P.A. van Hal, E.C.P. Smits, T.C.T. Geuns, H.B. Akkerman, B.C. de Brito, S. Perissinotto, G. Lanzani, A.J. Kronemeijer, V. Geskin, J. Cornil, P.W.M. Blom, B. de Boer, D.M. de Leeuw, *Nat. Nanotechnol.* **2008**, *3*, 749-754.

85. J. Liao, L. Bernard, M. Langer, C. Schönenberger, M. Calame, *Adv. Mater.* **2006**, *18*, 2444-2447.

86. J. Liao, M.A. Mangold, S. Grunder, M. Mayor, C. Schönenberger, M. Calame, *New J. Phys.* **2008**, *10*, 065019.

87. L. Bernard, Y. Kamdzhilov, M. Calame, S.J. van der Molen, J. Liao, C. Schönenberger, *J. Phys. Chem. C* **2007**, *111*, 18445-18450.

88. S.J. van der Molen, J. Liao, T. Kudernac, J.S. Agustsson, L. Bernard, M. Calame, B.J. van Wees, B.L. Feringa, C. Schönenberger, *Nano Lett.* **2009**, *9*, 76-80.

89. J. Liao, J.S. Agustsson, S. Wu, C. Schönenberger, M. Calame, Y. Leroux, M. Mayor, O. Jeannin, Y. Ran, S. Liu, S. Decurtins, *Nano Lett.* **2010**, *10*, 759-764.

90. E.A. Osorio, T. Bjørnholm, J.-. Lehn, M. Ruben, H.S.J. van der Zant, *J. Phys.: Condens. Matter* **2008**, *20*, 374121.

91. C.A. Martin, J.M. van Ruitenbeek, H.S.J. van der Zant, *Nanotechnology* **2010**, *21*, 265201.

92. E.H. van Dijk, D.J.T. Myles, M.H. van der Veen, J.C. Hummelen, *Org. Lett.* **2006**, *8*, 2333-2336.

93. U.H.F. Bunz, *Chem. Rev.* **2000**, *100*, 1605-1644.

94. F. Silvestri, A. Marrocchi, M. Seri, C. Kim, T.J. Marks, A. Facchetti, A. Taticchi, *J. Am. Chem. Soc.* **2010**, *132*, 6108-6123.

95. J.M. Tour, *Chem. Rev.* **1996**, *96*, 537-553; J.M. Tour, *Acc. Chem. Res.* **2000**, *33*, 791-804; J.M. Tour, A.M. Rawlett, M. Kozaki, Y. Yao, R.C. Jagessar, S.M. Dirk, D.W. Price, M.A. Reed, C. Zhou, J. Chen, W. Wang, I. Campbell, *Chem.-Eur. J.* **2001**, *7*, 5118-5134.

96. M. Mayor, H. Weber, *Chimia* **2002**, *56*, 494-499.

97. The density of OPE thiols on gold is estimated to be $4 \cdot 10^6$ μm^{-2}; Yang, Y. Qian, C. Engtrakul, L. Sita, G. Liu, *J.Phys.Chem.B* **2000**, *104*, 9059-9062.